PHYSICAL REVIEW LETTERS

Ion-Specific Anomalous Electrokinetic Effects in Hydrophobic Nanochannels

David M. Huang, Cécile Cottin-Bizonne, Christophe Ybert, and Lydéric Bocquet*

Université de Lyon, Université Lyon 1, LPMCN, and CNRS, UMR 5586, F-69622 Villeurbanne Cedex, France
(Received 22 December 2006; published 26 April 2007)

We show with computer simulations that anomalous electrokinetic effects, such as ion specificity and nonzero zeta potentials for uncharged surfaces, are generic features of electro-osmotic flow in hydrophobic channels. This behavior is due to the stronger attraction of larger ions to the ''vapor-liquidlike'' interface induced by a hydrophobic surface. We propose an analytical model involving a modified Poisson-Boltzmann description for the ion density distributions that quantitatively predicts the anomalous flow profiles. This description includes as a crucial component an ion-size-dependent hydrophobic solvation energy. These results provide an effective framework for predicting ion-specific effects, with potentially important implications for biological modeling.

Hydrophobic surfaces are at the origin of many surprising and potentially useful effects [1], such as hydrodynamic slippage [2,3] and the formation of nanobubbles [4] at surfaces. A common feature underlying many of these phenomena is the formation of a layer of depleted water density near the surface [5]—a vapor layer in the case of extremely hydrophobic surfaces. Vapor-liquid interfaces have been found in recent spectroscopic experiments [6] and computer simulations [7] to attract large and polarizable ions such as Br^- and I^- but not small ions such as Na^+ and Cl^-. This ion-specific behavior, contrary to traditional theories of electrolyte interfaces, which account only for differences in ion valency [8], is behind the substantial dependence on anion type of the surface tension of aqueous solutions of halide salts [9]. Just as ion specificity affects equilibrium properties of vapor-liquid interfaces like surface tension, a similarly important role is expected for dynamic phenomena near the ''vapor-liquidlike'' interfaces induced by hydrophobic surfaces. The implications are considerable for fluid transport in microfluidic ''lab-on-chip'' devices [10], for which surface effects are predominant and electrokinetic techniques for driving flows widely used, and for modeling biological systems [1], in which ion-specific Hofmeister series are ubiquitous [11].

In this work, we investigate by computer simulations the anomalous electrokinetic effects that arise in electro-osmotic (EO) flow through hydrophobic channels due to interfacial ion specificity. We also develop a simple model, comprising continuum hydrodynamic equations and a modified Poisson-Boltzmann (PB) description for the ion density distributions, which is able to predict accurately the effects of ion specificity on the simulated EO flow profiles and zeta potentials and points, moreover, to the crucial role of the hydrophobic solvation energy. Our analytic theory is a powerful tool for describing ion-specific effects and their consequences for dynamics.

The system studied comprised an aqueous solution of monoatomic monovalent salt ions confined between two parallel solid walls. 2160 fluid molecules in total were used in all cases, and the extended simple point charge (SPC/E) [12] model was employed for the aqueous solvent. Each wall was composed of 648 atoms arranged in three unit cell layers of an fcc lattice oriented in the ⟨100⟩ direction [lateral dimensions (x, y): 48.21×32.14 Å^2]. To model charged surfaces, identical charges were added to each of the atoms in the top solid layer in contact with the fluid. The interwall distance was adjusted so that the average pressure, defined by the force per unit area on the solid atoms, was approximately 10 atm in equilibrium simulations. Periodic boundary conditions were applied in the x and y directions, while empty space was added in the z direction so that the total system was 3 times as large as the primary simulation cell, which was centered at $z = 0$.

Simulations were carried out with the LAMMPS [13] molecular dynamics package. Bond length and angle constraints for the rigid water molecules were enforced with the SHAKE algorithm, and a constant temperature of 298 K was maintained with a Nosé-Hoover thermostat (applied only to degrees of freedom in the y direction in the flow simulations, for flow along x). Electrostatic interactions were calculated with the particle-particle particle-mesh method, with a correction applied to remove the dipolar interactions between periodic replicas in the z direction. Short-ranged van der Waals interactions between particles were modeled with the Lennard-Jones (LJ) potential, $v_{ij}(r_{ij}) = 4\varepsilon_{ij}[(\sigma_{ij}/r_{ij})^{12} - (\sigma_{ij}/r_{ij})^6]$ for an interparticle separation of r_{ij} and particle types i and j [$\sigma_{ij} = (\sigma_{ii} + \sigma_{jj})/2$ and $\varepsilon_{ij} = \sqrt{\varepsilon_{ii}\varepsilon_{jj}}$]. All LJ interactions were truncated and shifted to zero at 10 Å. For the solid atoms, LJ parameters were chosen to create a physically reasonable, albeit idealized, surface: We took $\sigma_{ss} = 3.37$ Å, used a close-packed density $\rho_s = \sigma_{ss}^{-3}$, and chose $\varepsilon_{ss} = 0.164$ and 2.08 kcal/mol to create, respectively, a hydrophobic and a hydrophilic surface, as characterized by the contact angle of a water droplet on uncharged surfaces of roughly 140 and 55°.

EO flow of solutions of either NaI or NaCl were studied, the only difference between the two cases being anion size. Except for one case, we used ion LJ parameters from Ref. [14]: We chose $\sigma_{ii} = 6.00$ Å for I⁻ (instead of 5.17 Å) to reproduce approximately liquid-vapor interfacial ion densities measured in simulations of NaI-water solutions of similar concentration but using more complex polarizable force fields [7]. Our simulated density profiles are shown in Fig. 1(c). Although ion polarizability plays a role in stabilizing I⁻ at the air-water interface [7], simulations have shown that the dominant contribution to the stabilization free energy is associated with creating an uncharged ion-sized cavity in the fluid and adding the permanent charge to the cavity [15], which are accounted for in this work. Thus, we regard our simple parametrization of the I⁻ LJ diameter, coupled with the use of nonpolarizable force fields, as adequate for the purpose of capturing the dynamic consequences of the experimentally observed interfacial enhancement of I⁻.

The effects of anion size and surface wettability on interfacial ion densities are illustrated in Fig. 1. While Cl⁻ is not found near the hydrophobic surface in Fig. 1(b), Fig. 1(a) shows a substantially enhanced interfacial I⁻ concentration. No such enhancement is seen for I⁻ ions near the hydrophilic surface [Fig. 1(d)] even though the direct ion-solid interactions are stronger in this case, indicating that the ion density profiles arise largely due to the water structure induced by the surface.

EO flow was induced in our simulations by applying an electric field E_x of 0.05–0.4 V/nm in the x direction (linear response to the applied force was verified for all reported results). Starting from an initial random configuration with zero total linear momentum, simulations were run for roughly 10 ns, with statistics collected only after reaching the steady state (typically 1 ns). Surface charge densities Σ of 0, ± 0.031, and ± 0.062 C/m² and electrolyte concentrations of approximately $0.2M$ and $1M$ (8 and 40 ion pairs, respectively, for $\Sigma = 0$) were studied.

The measured velocity $v_x(z)$ is shown in Fig. 2 for the $1M$ solutions in hydrophobic channels with $\Sigma = 0$ and ± 0.062 C/m²; it has been scaled by the bulk viscosity η, bulk dielectric constant ϵ, and applied electric field E_x for ease of comparison with the zeta potential, defined in terms of the velocity in the channel center as $\zeta \equiv -\eta v_x(0)/(\epsilon_0 \epsilon E_x)$, where ϵ_0 is the vacuum permittivity. For ϵ, we used the dielectric constant of pure SPC/E water under similar thermodynamic conditions, $\epsilon_w = 68$ [16]. The ζ potentials for all of the surface charges are given in Fig. 3.

Figures 2 and 3 clearly show the sensitivity of the EO flow to anion type, particularly for the neutral and positively charged surfaces. (The flow for the negatively charged surfaces is dominated by the excess of cations, Na⁺ in all simulations.) A noteworthy point is the measurement of a nonzero ζ potential ($\zeta \simeq -40$ mV) for the neutral hydrophobic channel with a solution of NaI, even though the total electrostatic force exerted on the charge-neutral fluid is zero. This is in strong contrast to the traditional theory of the electric double layer [8], though observed in previous experiments [17,18] and computer simulations [19]. By contrast, ζ for NaCl in the same channel was negligible. Our measured ζ potentials of 0 and -38 mV, respectively, for $1M$ NaCl and NaI are consistent with experimental surface potentials of roughly 0 and -20 mV, respectively, for vapor-liquid interfaces of the same solutions [20]; ζ for NaI is also of similar magnitude to the value of -9 mV measured by electrophoresis of neutral liposomes in $1M$ KI [18], for which ion-specific effects should be smaller due to the greater simi-
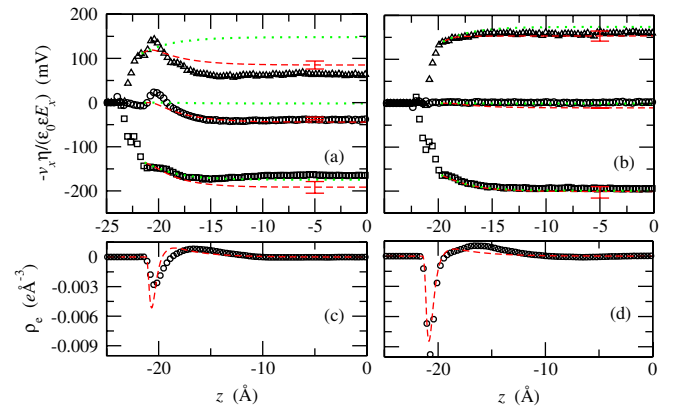
FIG. 2 (color online).   Top: Velocity profiles in a hydrophobic channel for $\Sigma = -0.062$, 0, and $+0.062$ C/m² (from bottom to top) with (a) [NaI] $\approx 1M$ and (b) [NaCl] $\approx 1M$. The simulation results (symbols) are compared with solutions of the modified PB equation using (see text for details) the SP model (dashed lines) and the SP model with $U_{hyd}^\pm = 0$ (dotted lines). Typical error bars for the theoretical curves are shown. Error bars in the simulated velocities are roughly the size of the points. Bottom: Ionic charge density profile $\rho_e(z)$ for [NaI] $\approx 1M$ with (c) $\Sigma = 0$ and (d) $\Sigma = +0.062$ C/m². The symbols are from simulation. The lines are solutions of the modified PB equation with the SP model.
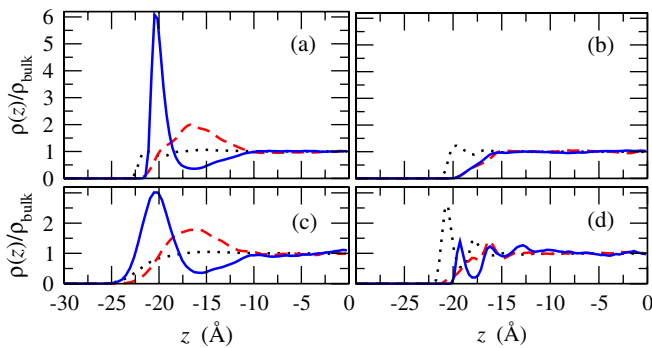

FIG. 1 (color online).   Simulated density profiles of negative ions (solid lines), positive ions (dashed lines), and water (dotted lines) for roughly $1M$ solutions of (a) NaI and (b) NaCl between neutral hydrophobic surfaces, (c) NaI at a vapor-liquid interface, and (d) NaI between neutral hydrophilic surfaces.
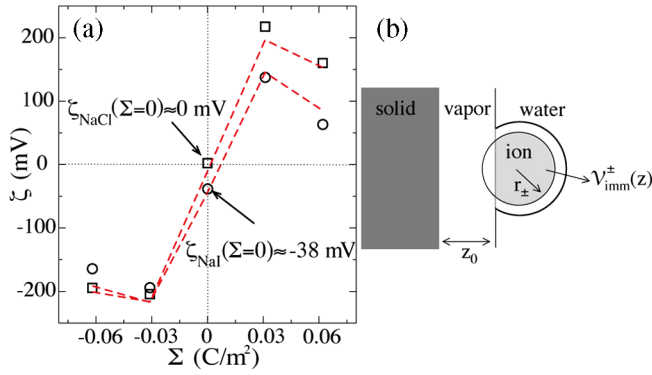
FIG. 3 (color online).   (a) Zeta potential of the hydrophobic surface versus surface charge for $1M$ solutions of NaI and NaCl [simulation: NaI (circles); NaCl (squares)]. The lines are solutions of the Stokes equation with ρ_e from solving the PB equation using the step-polarization model (see text). Error bars in the simulated ζ are roughly the size of the points. (b) Schematic of an ion at the solid-liquid interface, illustrating the origin of $U_{\text{hyd}}^{\pm}$ and its calculation.

larity in size of K^+ and I^- compared with Na^+ and I^-. Although not shown in Fig. 3, we found that ζ for $\Sigma = 0$ was not sensitive to electrolyte concentration. Also, ζ was insignificant for NaI in the neutral hydrophilic channel.

The anomalous result for the uncharged walls can be understood in terms of continuum hydrodynamics, in which the EO flow is described by the Stokes equation [8] $d^2 v_x(z)/dz^2 = -(E_x/\eta)\rho_e(z)$, where $\rho_e(z) = e[\rho_+(z) - \rho_-(z)]$ is the total charge density due to cations or anions of number density $\rho_{\pm}(z)$, and e is the elementary charge. Exploiting our system's symmetry about $z = 0$ and integrating the Stokes equation twice with boundary conditions (BCs) $v_x|_{z=z_h} = b(dv_x/dz)|_{z=z_h}$ and $(dv_x/dz)|_{z=0} = 0$, where b is the slip length applied at the hydrodynamic boundary z_h [3], gives

$$\zeta \equiv -\frac{\eta v_x(0)}{\epsilon_0 \epsilon_w E_x} = -\frac{1}{\epsilon_0 \epsilon_w} \int_{z_h}^{0} dz'(z' - z_h + b)\rho_e(z'). \quad (1)$$

According to Eq. (1), ζ is proportional to the first moment of the charge distribution ρ_e relative to an origin at the shear plane $z_s = z_h - b$ (the plane where the nonslip BC applies). Unless $\rho_e(z) = 0$ everywhere, this quantity will generally be nonzero even if the total charge $\int_{z_h}^{0} dz' \rho_e(z')$ is zero, as is the case for NaI near the uncharged hydrophobic wall due to the differing propensities of Na^+ and I^- for the surface. It has been suggested that such a nonzero ζ potential occurs for some noncharged surfaces due to ion-specific "binding" [18], to the presence of an immobile interfacial layer of charge [17] or, more generally, to a reduced mobility in the interfacial layer [19]. In contrast, our present results show that ζ will be nonzero even if all of the charge is fully mobile. Another interesting consequence of Eq. (1) is that, as long as b is finite, surface slippage makes no contribution to the velocity of a charge-

neutral fluid containing only mobile charges: i.e., the system behaves as if $b = 0$ and the flow is independent of the solid-fluid friction. In fact, global fluid neutrality requires that the wall-to-fluid force vanish in the steady state, which imposes both a vanishing slip velocity and a vanishing velocity gradient at the wall (see Fig. 2 for $\Sigma = 0$). In this respect, the case where b is infinite appears singular as the velocity at z_h need not vanish: The velocity is determined by momentum conservation as momentum cannot be transferred to a frictionless surface, and in the end no net flow is achieved (not shown).

So far, we have presented a general explanation for the observed ion-specific electrokinetic effects; however, of additional practical value would be a model capable of quantitatively predicting the ion density and EO velocity profiles. With this aim, we have sought to construct the minimal physically accurate model for ρ_e for use in the Stokes equation for v_x. To obtain ρ_e, we solved the one-dimensional Poisson equation [8] $\frac{d}{dz}[-\epsilon_0 \frac{d}{dz} V(z) + P(z)] = \rho_e(z)$, with Neumann BCs applied at the position z_w of the surface charge and a mean-field approximation for the ion densities $\rho_{\pm}(z) = \rho_0 \exp\{-\beta[\pm eV(z) + U_{\text{ext}}^{\pm}(z)]\}$, where ρ_0 is the bulk ion density and $U_{\text{ext}}^{\pm}$ is an external potential acting on the ions due to interactions other than the electrical potential V. For the polarization of the medium P, we assumed $\epsilon(z)$ to have a step-function behavior (from 1 to ϵ_w) at the vapor-liquid interface so that $P(z) = -\epsilon_0[\epsilon_w - 1]\frac{dV(z)}{dz}$ for $z \geq z_0$ and $P = 0$ otherwise, with z_0 the position of the first peak in the simulated water oxygen density distribution function ["step-polarization" (SP) model].

For the external potential, we used the sum of three components: $U_{\text{ext}}^{\pm} = U_{\text{image}}^{\pm} + U_{\text{wall}}^{\pm} + U_{\text{hyd}}^{\pm}$. The first two terms $U_{\text{image}}^{\pm}$ and $U_{\text{wall}}^{\pm}$ are, respectively, the image potential acting on the ions due to the dielectric interface at z_0 [Eq. (3) in Ref. [9]] and the ion-solid LJ interaction, obtained by integrating the interparticle LJ interaction over a uniform density ρ_s of solid atoms occupying the $z \leq z_w$ half-plane. The final term $U_{\text{hyd}}^{\pm}$ is the free energy to create an ion-sized cavity in the fluid, i.e., to solvate a solute with no attraction to the solvent. This hydrophobic solvation energy has generally been ignored in calculations of interfacial ion densities, since it is negligible compared with electrostatic interactions for typical small ions such as Na^+ or Cl^-. We took $U_{\text{hyd}}^{\pm}$ to be proportional to the volume $\mathcal{V}_{\text{imm}}^{\pm}$ (which is the appropriate scaling for the solute sizes studied [21]) of the ion immersed in the liquid in the $z \geq z_0$ half-plane [see Fig. 3(b)]:

$$U_{\text{hyd}}^{\pm}(z) = C_0[\mathcal{V}_{\text{imm}}^{\pm}(z) - \mathcal{V}_{\text{ion}}^{\pm}], \quad (2)$$

with $\mathcal{V}_{\text{ion}}^{\pm}$ the total volume of the ion of solvent-excluded radius $r_{\pm}$. We took $r_{\pm}$ from bulk simulations of ions in water as the radius at which the ion-water radial distribution function fell to $1/e$ of its bulk value (2.24, 2.98, and 3.73 Å, respectively, for Na^+, Cl^-, and I^-). For the pro-

portionality constant $C_0 = 2.8 \times 10^8$ J/m^3, we used the solvation free energy per unit volume measured under similar thermodynamic conditions in simulations of hard-sphere solutes of radius 0–5 Å in SPC/E water [21]. We omitted a final plausible term in $U_{\text{ext}}^\pm$, the Born solvation energy $U_{\text{Born}}^\pm$ for charging the ion-sized cavity, as we found it made little difference to our results, at least using a simple expression employed by Boström *et al.* [9].

The Stokes equation was solved using the calculated $\rho_e(z)$ and η and b measured independently in Poiseuille and Couette flow simulations, respectively [22]. For $\Sigma = 0$, we used $b = 0$, as justified above. BCs were applied in all cases at the position z_h of the first peak in the simulated water oxygen density distribution function [23]. As a test of the validity of the continuum hydrodynamic description, we solved the Stokes equation using the exact $\rho_e(z)$ from our simulations and found almost perfect agreement with the simulated velocity profiles (not shown). Both the charge density profile $\rho_e(z)$ and velocity profiles calculated from the modified PB theory described above with the full $U_{\text{ext}}^\pm$ are in good agreement with the simulated results, as shown in Fig. 2. The resulting prediction for the ζ potential reproduces very well, both qualitatively and quantitatively, the simulation results, as shown in Fig. 3. It should be noted that the nonmonotonic behavior of ζ as a function of Σ in Fig. 3 is due to the decrease in the slip length b with Σ. Note that it is possible to replace the SP model for $P(z)$ by the exact value of the polarization (the gradient of which is equal to minus the charge density due to water in our simulations): Doing so yields an even better agreement of the predicted ζ potentials with simulation results (not shown) but at the expense of using the simulated water charge density profile as an input. Finally, when $U_{\text{hyd}}^\pm$ is neglected, the calculated ion density profiles and velocities are significantly wrong for the neutral and positively charged surfaces (see Fig. 2), pointing to the crucial role of the hydrophobic solvation energy. This is not an issue for the negatively charged surfaces, since the flow is dominated by Na$^+$, for which U_{hyd}^+ is negligible. Although not shown, we found that the conventional theory of the electric double layer, which assumes $\epsilon(z) = \epsilon_w$ and $U_{\text{ext}}^\pm = 0$ everywhere, performed very poorly in almost all cases.

In summary, we have shown that anomalous electrokinetic effects such as nonzero ζ potentials for uncharged surfaces are generic features of EO flow in hydrophobic channels when the dissolved cation and anion differ substantially in size. We have also developed a simple model, comprising continuum hydrodynamic equations and a modified PB description for the ion densities, which accurately predicts the simulated flow profiles. We have found that the incorporation in the model of an ion-size-dependent hydrophobic solvation energy, which favors interfacial enhancement of large ions, is crucial to reproducing the ion-specific effects observed in the simulations. This analytic theory, which is able to capture the subtle and complex effects of the interfacial specificity of ions, provides a useful framework for modeling biological systems, in which Hofmeister series are ubiquitous [11].

*Electronic address: lyderic.bocquet@univ-lyon1.fr

[1] D. Chandler, Nature (London) **437**, 640 (2005).
[2] E. Lauga, M. P. Brenner, and H. A. Stone, in *Handbook of Experimental Fluid Dynamics*, edited by J. Foss, C. Tropea, and A. Yarin (Springer, New York, 2005).
[3] L. Joly, C. Ybert, E. Trizac, and L. Bocquet, Phys. Rev. Lett. **93**, 257805 (2004).
[4] P. Attard, Adv. Colloid Interface Sci. **104**, 75 (2003).
[5] R. R. Netz, Curr. Opin. Colloid Interface Sci. **9**, 192 (2004).
[6] S. Ghosal *et al.*, Science **307**, 563 (2005).
[7] L. Vrbka *et al.*, Curr. Opin. Colloid Interface Sci. **9**, 67 (2004).
[8] R. J. Hunter, *Foundations of Colloid Science* (Oxford University, Oxford, 2001), 2nd ed.
[9] M. Boström, W. Kunz, and B. W. Ninham, Langmuir **21**, 2619 (2005).
[10] T. Squires and S. Quake, Rev. Mod. Phys. **77**, 977 (2005).
[11] M. Boström, D. R. M. Williams, and B. W. Ninham, Phys. Rev. Lett. **87**, 168103 (2001).
[12] H. J. C. Berendsen, J. R. Grigera, and T. P. Straatsma, J. Phys. Chem. **91**, 6269 (1987).
[13] S. J. Plimpton, J. Comput. Phys. **117**, 1 (1995); LAMMPS: http://lammps.sandia.gov.
[14] S. Koneshan, J. C. Rasaiah, R. M. Lynden-Bell, and S. H. Lee, J. Phys. Chem. B **102**, 4193 (1998).
[15] G. Archontis and E. Leontidis, Chem. Phys. Lett. **420**, 199 (2006).
[16] P. Höchtl, S. Boresch, W. Bitomsky, and O. Steinhauser, J. Chem. Phys. **109**, 4927 (1998).
[17] A. Dukhin, S. Dukhin, and P. Goetz, Langmuir **21**, 9990 (2005).
[18] H. I. Petrache, T. Zemb, L. Belloni, and V. A. Parsegian, Proc. Natl. Acad. Sci. U.S.A. **103**, 7982 (2006).
[19] S. Joseph and N. R. Aluru, Langmuir **22**, 9041 (2006).
[20] H. L. Jarvis and M. A. Scheiman, J. Phys. Chem. **72**, 74 (1968).
[21] D. M. Huang, P. L. Geissler, and D. Chandler, J. Phys. Chem. B **105**, 6704 (2001).
[22] We obtained η from independent Poiseuille flow simulations: $\eta_w = 0.65 \pm 0.06$, 0.75 ± 0.04, and 0.89 ± 0.04 mPa s, respectively, for pure SPC/E water, 1M NaI, and 1M NaCl. From Couette flow simulations, we obtained b as the distance beyond z_h at which the linearly extrapolated fluid velocity was equal to the wall velocity: $b \approx 35$ and 15 Å (errors roughly ± 1.1 and ± 0.4 Å), respectively, for $\Sigma = \pm 0.031$ and ± 0.062 C/m^2, with a slight dependence on electrolyte type for 1M solutions.
[23] Changing the definition of z_h results in no change to $\upsilon_x(z)$ if $\rho_e(z) = 0$ for $z < z_h$; we also found that our chosen definition resulted in consistent values for b from Couette and Poiseuille flow simulations.